Laminar Hypersonic Boundary Layer Manipulation via MHD-Leveraging Devices

Joseph D. Franciamore
Rensselaer Polytechnic Institute

Aviation 2024, July 31st

Plan for the Presentation

- Introduction to MHD control methods.
- Importance and applicability of the MHD boundary layer.
- Modeling an N-component hypersonic plasma with chemical reactions.
- Pseudo-Couette preliminary analysis.
- Numerical validation of Pseudo-Couette analytical results.
- A look at high fidelity hypersonic MHD simulation with boundary layer profile outlook.
- Concluding design considerations.

Introduction to MHD Control

- Magnetohydrodynamic (MHD) control via Lorentz forces.
- Relies on post-shock plasma.
- Blunt-nosed bodies.
- SSTO, Atmospheric Entry Vehicles, Scramjet Inlet Control, Thermal Protection.
- Experiments and numerical studies have demonstrated viability.
- Entropy gradient, Crocco's theorem, topology change.

- Shear stress determination and composition control.
- Dampening of turbulent effects, Laminarization.

$$\vec{\mathbf{J}} = \sigma(\vec{\mathbf{E}} + \vec{\mathbf{V}} \times \vec{\mathbf{B}})$$

$$\vec{\mathfrak{F}} = \vec{\mathbf{J}} \times \vec{\mathbf{B}}$$

Vehicle Types Benefiting From Boundary Layer Control

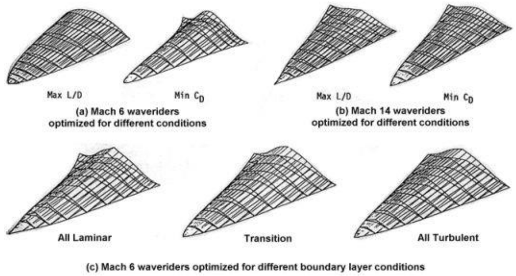

Bowcutt, Kevin G., John D. Anderson, and Diego Capriotti. "Viscous optimized hypersonic waveriders." *25th AIAA Aerospace Sciences Meeting*. 1987.

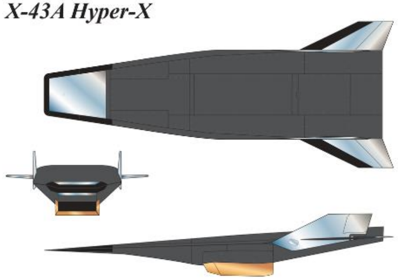

X-43A Color 3 View. 16 Jan. 2014. *NASA*, National Aeronautics and Space Administration, https://www.nasa.gov/image-article/x-43a-color-3-view/. Accessed 14 July 2024.

Falcon HTV-2. *DARPA*, Defense Advanced Research Projects Agency. Accessed 14 July 2024.

Modeling an N-Component Weakly Ionized Plasma

- A post-shock plasma consisting of N species must be modeled via a mass-averaged velocity term to produce equations that are computationally viable.
- Mass continuity for the i^{th} species

$$\frac{\partial \rho_i}{\partial t} + \nabla \bullet \left(\rho_i \vec{\mathbf{V}}_i\right) = -\nabla \bullet \vec{\boldsymbol{\Psi}}$$

- Charge continuity for the i^{th} species

$$\frac{\partial \rho_{qi}}{\partial t} + \nabla \bullet \vec{\mathbf{J}}_i = -\nabla \bullet \vec{\psi}$$

- Momentum conservation for the i^{th} species

$$\frac{\partial (\rho_i \vec{\mathbf{V}}_i)}{\partial t} + \left(\vec{\mathbf{V}}_i \bullet \nabla\right) \vec{\mathbf{V}}_i = \nabla \bullet \mathbb{P}_i + \rho_{qi} \vec{\mathbf{E}} + \vec{\mathbf{J}}_i \times \vec{\mathbf{B}} + \nu_{ij} \left(\vec{\mathbf{V}}_i - \vec{\mathbf{V}}_j\right)$$

Modeling an N-Component Weakly Ionized Plasma

$$\vec{\mathbf{V}} = \frac{\Sigma_{i=1}^{N} m_i \vec{\mathbf{V}}_i}{\Sigma_{i=1}^{N} m_i}$$

$$\rho\frac{Du}{Dt} = -\frac{\partial p}{\partial x} + \frac{\partial \tau_{xx}}{\partial x} + \frac{\partial \tau_{yx}}{\partial y} + \frac{\partial \tau_{zx}}{\partial z} + \sigma((\vec{\mathbf{V}} \times \vec{\mathbf{B}}) \times \vec{\mathbf{B}}))_x$$

$$\rho\frac{Dv}{Dt} = -\frac{\partial p}{\partial y} + \frac{\partial \tau_{xy}}{\partial x} + \frac{\partial \tau_{yy}}{\partial y} + \frac{\partial \tau_{zy}}{\partial z} + \sigma((\vec{\mathbf{V}} \times \vec{\mathbf{B}}) \times \vec{\mathbf{B}}))_y$$

$$\rho\frac{Dw}{Dt} = -\frac{\partial p}{\partial z} + \frac{\partial \tau_{xz}}{\partial x} + \frac{\partial \tau_{yz}}{\partial y} + \frac{\partial \tau_{zz}}{\partial z} + \sigma((\vec{\mathbf{V}} \times \vec{\mathbf{B}}) \times \vec{\mathbf{B}}))_z$$

$$\frac{\partial \rho}{\partial t} + \nabla \bullet \left(\rho \vec{\mathbf{V}}\right) = 0$$

$$\frac{\partial \rho_q}{\partial t} + \nabla \bullet \vec{\mathbf{J}} = 0$$

- Equations may be unified via mass-averaging.
- Eliminates inter-species collision.

Pseudo-Couette Hypersonic Boundary Layer

- At high Mach numbers $\theta \approx \beta$.
- Thin shock layer interacts with boundary layer.
- Oblique wave driving wall.
- Couette boundary conditions enable for approximation of flow alterations.
- Constant property approximation in post-shock environment.

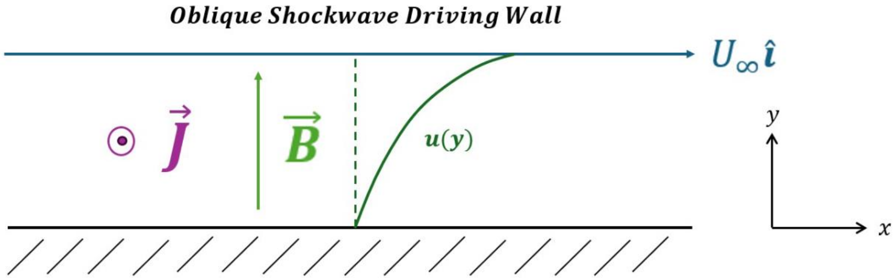

$$\mu \frac{\partial^2 u}{\partial y^2} = \sigma B^2 u$$

$$\frac{\partial p}{\partial y} = 0$$

$$k \frac{\partial^2 T}{\partial y^2} + \mu \frac{\partial}{\partial y}\left(u \frac{\partial u}{\partial y}\right) = \sigma B^2 u^2$$

Solving the Equations

$$u(y) = \phi e^{B\sqrt{\frac{\sigma}{\mu}}y} - \psi e^{-B\sqrt{\frac{\sigma}{\mu}}y}$$

$$u(0) = 0$$

$$u(D) = U_\infty$$

$$u(y) = U_\infty \left(e^{BD\sqrt{\frac{\sigma}{\mu}}} - e^{-BD\sqrt{\frac{\sigma}{\mu}}}\right)^{-1} \left(e^{B\sqrt{\frac{\sigma}{\mu}}y} - e^{-B\sqrt{\frac{\sigma}{\mu}}y}\right)$$

$$\frac{u(y)}{U_\infty} = \left(e^{\mathfrak{H}} - e^{-\mathfrak{H}}\right)^{-1} \left(e^{\frac{\mathfrak{H}}{D}y} - e^{-\frac{\mathfrak{H}}{D}y}\right)$$

$$\mathfrak{H} = BD\sqrt{\frac{\sigma}{\mu}}$$

$$\mathfrak{A} = \frac{\mathfrak{H}}{Re}$$

$$c_f = 4\mathfrak{A}\left(e^{\mathfrak{H}} - e^{-\mathfrak{H}}\right)^{-1}$$

$$\tau_{xy} = \mu \frac{\partial u}{\partial y}$$

Dimensionless Boundary Layer Profile

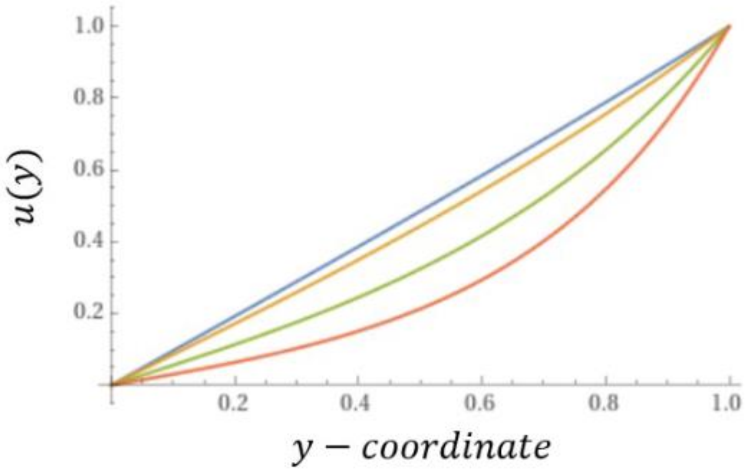

Dimensionless boundary layer profiles for $\mathfrak{H} = 0.5, 1, 2, 3$ in sequential order from left to right.

- Increased Hartmann numbers demonstrate significant alterations to the boundary layer.

$$\frac{u(y)}{U_\infty} \longleftrightarrow \mathcal{F}(\mathfrak{H})$$

$$\tau_w = 2U_\infty \frac{\mathfrak{H}\mu}{D}\left(e^{\mathfrak{H}} - e^{-\mathfrak{H}}\right)^{-1}$$

$$c_f = 4\mathfrak{A}\left(e^{\mathfrak{H}} - e^{-\mathfrak{H}}\right)^{-1}$$

$$\mathfrak{A} = \frac{\mathfrak{H}}{Re}$$

Numerical Validation

- mhdFoam solver, based on PISO algorithm.
- Structured rectangular mesh.
- Couette boundary conditions.
- Laminar flow.
- Magnetic field implemented.
- No pressure gradients.
- Incompressible.

Numerical Validation

•Ahrens, James, Geveci, Berk, Law, Charles, *ParaView: An End-User Tool for Large Data Visualization*, Visualization Handbook, Elsevier, 2005, ISBN-13: 9780123875822
•Ayachit, Utkarsh, *The ParaView Guide: A Parallel Visualization Application*, Kitware, 2015, ISBN 9781930934306

Dimensionless boundary layer profiles for $\mathfrak{H} = 0, 1, 2, 4, 6$ in sequential order from left to right.

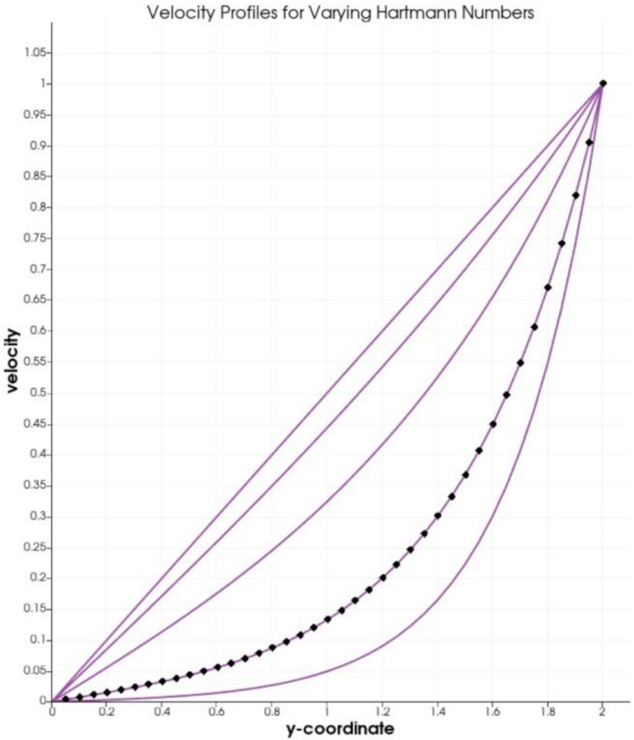

Transition to High Fidelity Numerical Methods

- Open source hy2Foam two-temperature chemically reacting CFD software coupled with MHD flux and source terms.
- Lorentz force, Joule heating.
- Low Re (m) assumption.
- Continuum regime, very small Knudsen number (continuum).
- Temperature power laws.
- Axisymmetric.

Mesh Details and Boundary Conditions

Geometric altitude of 29.4 km based on the 1959 ARDC model atmosphere.

$$p_\infty = 1300\ Pa$$

$$M_\infty = 28.712$$

$$T_\infty = 250\ K$$

$$T_{wall} = 300\ K$$

$$\rho_\infty = 0.0182\ \frac{kg}{m^3}$$

$$\chi_{N_2,\infty} = 0.7$$

$$\chi_{O_2,\infty} = 0.3$$

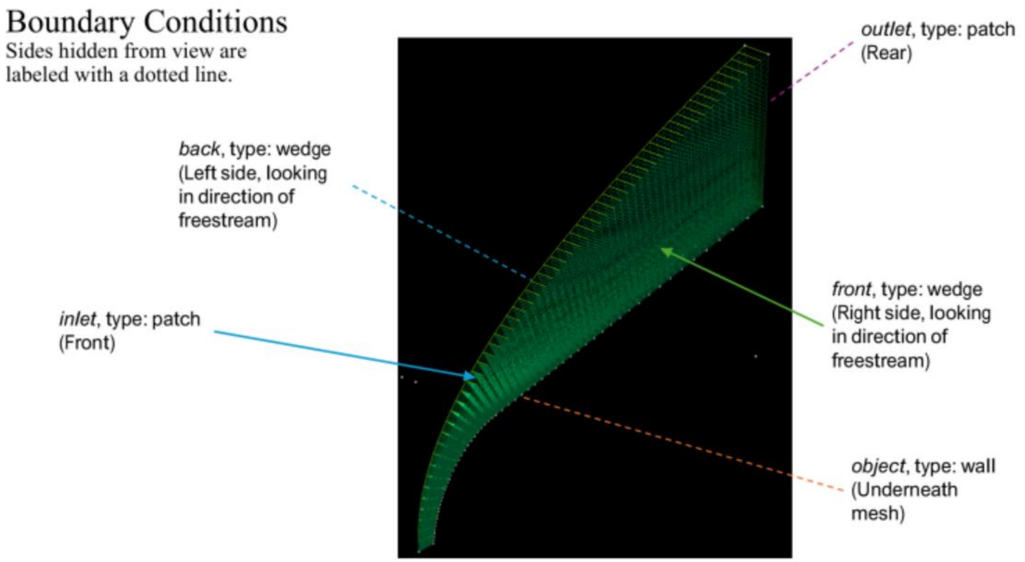

Electrical Conductivity Model

- Establishing a proper plasma electrical conductivity remains challenging in the analysis of MHD-Hypersonic interactions.
- Temperature-based models.
- Hybrid temperature-electron pressure models.

$$\sigma = \sigma_0 \cdot \left(\frac{T}{T_0}\right)^n$$

$$\sigma = 4.0227904 \cdot 10^{-18} \cdot \frac{n_{e^-}}{\sqrt{T}}$$

$$\sigma = 83.0 \cdot \exp\left(\frac{-3.6 \cdot 10^4}{T}\right)$$

$$\sigma = 1.56 \cdot 10^{-4} \cdot \frac{T^{1.5}}{\ln\left(1.23 \cdot 10^4 \cdot \frac{T^{1.5}}{\sqrt{n_{e^-}}}\right)}$$

Magnetic Field Calculation

Effective magnetic field strength of ~ 1.6 T

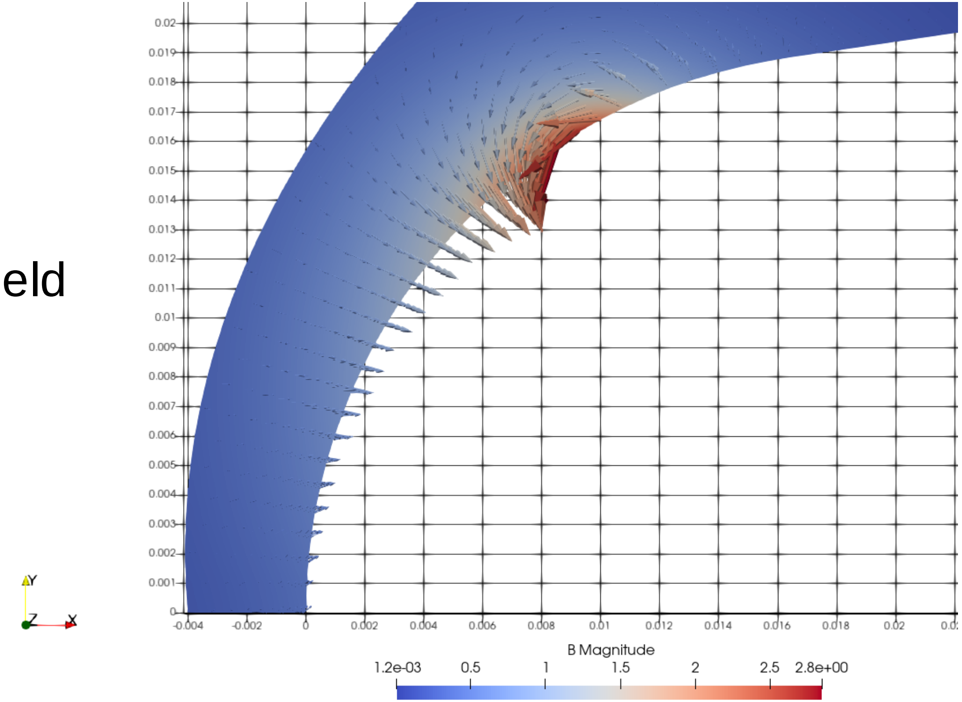

Scalar Value Maps

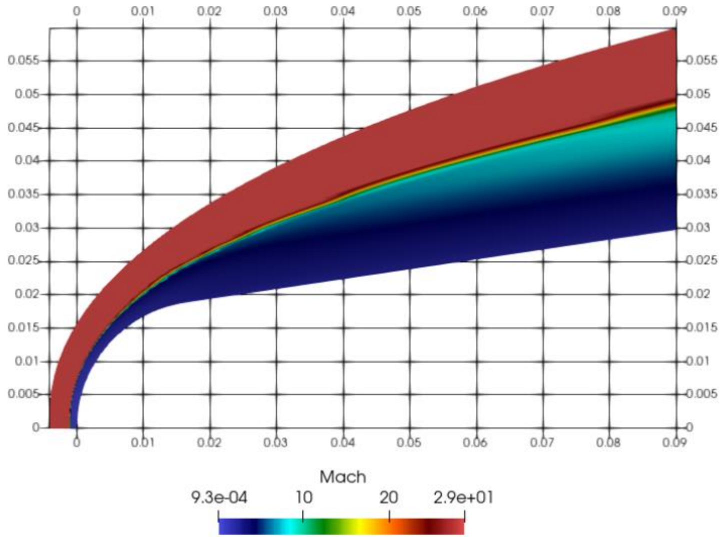

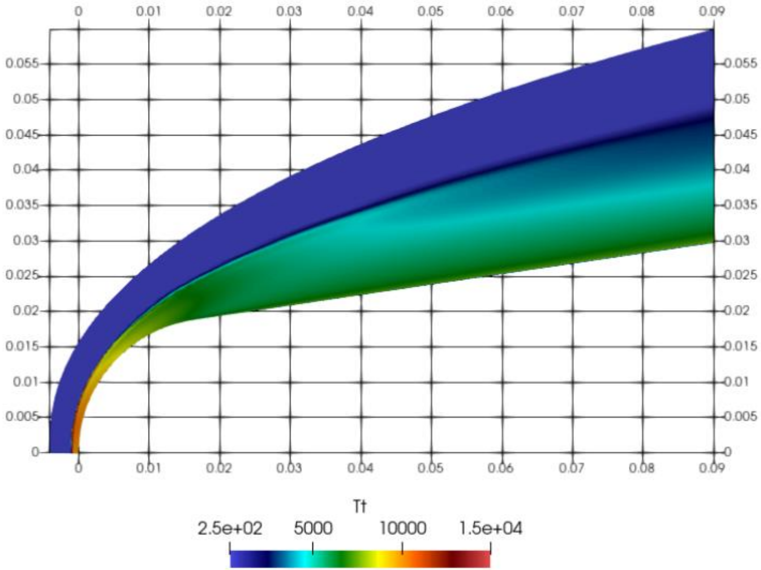

Surface Viscous Shear – NEW DATA

For the case offered by the University of Strathclyde, $\sigma_o = 5100\ \Omega^{-1}m^{-1}, T_0 = 12{,}000\ K, n = 2$

For the curve fit model based on theoretical gas calculations, $\sigma_o = 4100\ \Omega^{-1}m^{-1}, T_0 = 12{,}000\ K, n = 4$

Yos, Jerrold Moore. "Transport properties of nitrogen, hydrogen, oxygen and air to 30000 K." *Research and Advanced Development Division AVCO Corporation, Memorandum* 63 (1963).

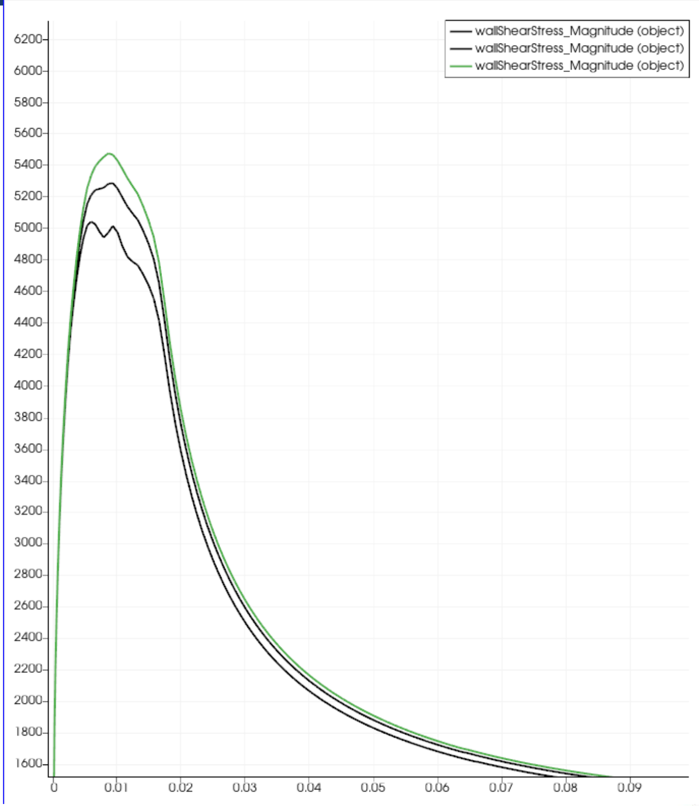

Pseudo-Couette Model: Regions of Applicability

Driving wall boundary layer approximation is only valid in select regions of the flow around a blunt-nosed body.

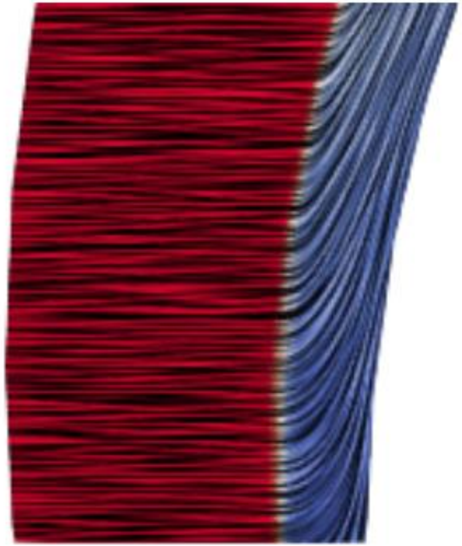

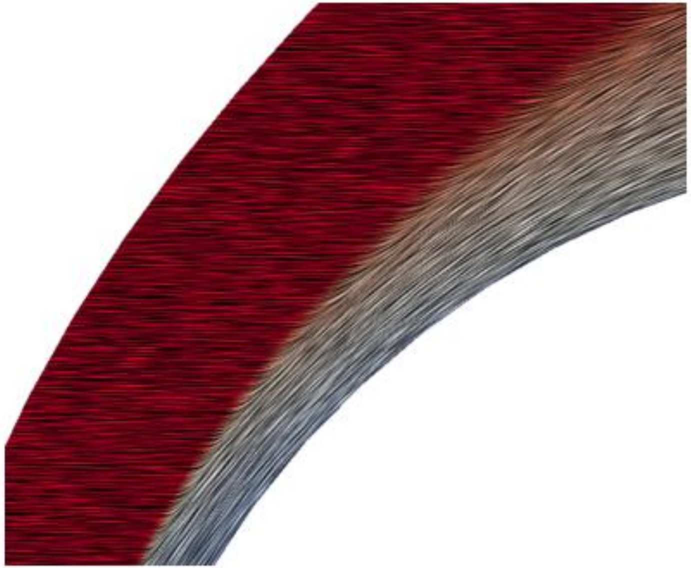

Numerically Derived Velocity Profile

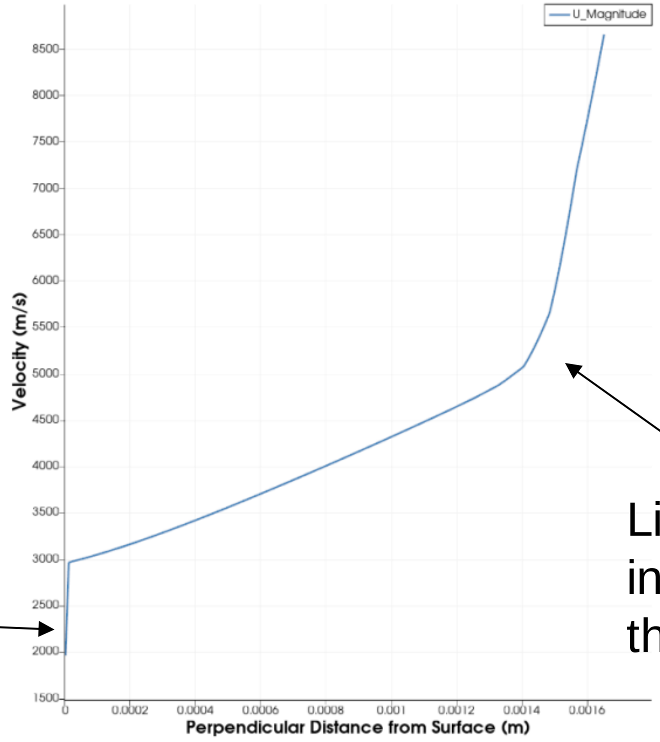

Wall slip is assumed to occur, potential numerical issue.

Linearity is invalidated close to the shock wave.

Methods of Enhancing MHD Interaction

- Alkali metal vapors.
- Supplementary ionic TPS systems.
- Surface electrodes
  - Numerous engineering challenges.
  - Challenging to implement for a reentry speed vehicle.
- Study Hall effect reduction.

Acknowledgements

The author sincerely thanks Dr. Ozgur Tumuklu for providing the necessary training and support required to make this project possible. The author also thanks RPI’s Center for Computational Innovations for its allocation of valuable computational resources.